Preferential solvation of Ca^{2+} in aqueous ammonia solution: Classical and combined *ab initio* quantum mechanical/ molecular mechanical molecular dynamics simulations

Anan Tongraar,*[a] Kritsana Sagarik[a] and Bernd Michael Rode[b]

[a] *School of Chemistry, Institute of Science, Suranaree University of Technology, Nakhon Ratchasima, 30000, Thailand. E-mail: anan@ccs.sut.ac.th*
[b] *Department of Theoretical Chemistry, Institute of General, Inorganic and Theoretical Chemistry, University of Innsbruck, Innrain 52a, A-6020, Innsbruck, Austria*

Received 29th August 2001, Accepted 30th November 2001
First published as an Advance Article on the web 8th January 2002

Classical and combined quantum mechanical/molecular mechanical (QM/MM) molecular dynamics simulations have been performed to investigate the solvation structure of Ca^{2+} in 18.4% aqueous ammonia solution. The classical molecular dynamics simulation has been carried out based on pairwise additive potentials. For the QM/MM scheme, the first solvation sphere of Ca^{2+} is treated by Born–Oppenheimer *ab initio* quantum mechanics using LANL2DZ basis sets, while the rest of the system is described based on classical pairwise additivity. The results indicate the importance of the QM treatment in obtaining a reliable geometrical arrangement as well as the correct coordination number of the solvated ion. Within the first solvation sphere of Ca^{2+}, the QM/MM simulation reveals a polyhedral structure with an average coordination number of 7.2, consisting of 5.2 water and 2 ammonia molecules, compared to the corresponding value of 9.7 composed of 6.7 water and 3 ammonia molecules obtained by classical pair potential simulation. The preference for ligands is discussed on the basis of detailed simulation results.

1. Introduction

Ion solvation in mixed solvent systems is an interesting phenomenon that plays an important role in solution chemistry and kinetics.[1] When ions interact with solvent species, substantial modification is caused in the local structure of the multi-component solvent mixture. The ability of ions to preferentially order the solvent components surrounding them and to form specific solvation complexes depends, *inter alia*, on the strength of the binding energy between the ions and the solvent molecules, and is usually discussed in terms of preferential solvation. The concept of preferential solvation of ions in a solvent mixture has been introduced to explain the variation in solution properties as a function of solvent composition.

Investigations of preferential solvation phenomena have been the subject of both experimental[2–6] and theoretical[5–10] studies. In general, the experimental observations can give good insight into the average structural and dynamical properties of ions in solutions.[2,11–15] However, particularly for an interpretation at the molecular level, they often lead to ambiguous results due to the limitations of the experimental techniques.[15–17] Theoretical investigations using Monte Carlo (MC) and molecular dynamics (MD) simulations provide an alternative way of elucidating the details of the solution structure.

In theoretical investigations, *ab initio* quantum mechanics is a well-known method of providing a correct treatment of systems at the molecular level. However, *ab initio* calculations for a condensed-phase system consisting of a large number of molecules are too time-consuming. Therefore, most previous and current MC and MD simulations on preferential ion solvation have relied on classical force fields,[5–10,18,19] in which the potential functions describing the inter- and intramolecular interactions of interacting atoms or molecules are constructed by fitting an analytical formula to a set of experimental data or to *ab initio* energy surface calculations. Obviously, for N-body systems, the proper potential functions should include all contributions of pair, three-body, four-body up to N-body interactions:

$$\begin{aligned} V_{\text{total}} &= \sum V_{\text{pair}} + \sum V_{3\text{-body}} + \sum V_{4\text{-body}} + \ldots + \sum V_{N\text{-body}} \\ &= \sum V_{ij}(r_i, r_j) + \sum V_{ijk}(r_i, r_j, r_k) \\ &\quad + \sum V_{ijkl}(r_i, r_j, r_k, r_l) + \ldots + \sum V_{ijkl\ldots N}(r_i, r_j, \ldots, r_N). \end{aligned} \tag{1}$$

The first term in eqn. (1) is known as the pairwise interaction and the remaining terms of the series are referred to as non-additive (or N-body) corrections. For a large system, the construction of potential functions including all interaction terms is hardly feasible due to the complicated orientation dependence of molecular systems containing 3, 4 or more species. On the other hand, the higher terms (three-, four-,..., N-body) often converge rather slowly and tend to have alternating signs.[20] It has been assumed, therefore, that the system's interactions are approximately equal to the summation of all pair interactions, *i.e.* the interaction between species i and j is defined as

$$V_{\text{pair}} = \sum_{i<j}^{N} V_{ij}(|r_i - r_j|) \tag{2}$$

where r_i and r_j are the position of species i and j, respectively. Although this approximation of pairwise additivity can yield reasonable results for the energetic data and the structural and dynamical properties of many systems, there are several cases where the importance of non-additive contributions for a

DOI: 10.1039/b107786d

correct description of the intermolecular interactions has been demonstrated.[21,22] In particular, for strongly interacting systems *e.g.* ion-containing solutions, it has been reported that the non-additive contributions always play a significant role and neglect of these terms results in the wrong geometrical arrangements and coordination numbers.[23–28]

Nowadays, as a result of the continuous increase in computer capacity and performance, more sophisticated and accurate simulation techniques incorporating quantum mechanical algorithms have become accessible. One of the recent approaches is the combined quantum mechanical and molecular mechanical method.[29,30] This technique has been applied to various condensed-phase systems.[31–38] A "Born–Oppenheimer *ab initio* QM/MM dynamics" technique has been employed to study the structural and dynamical properties of various ions in water and ammonia.[39–44] This technique treats the active-site region, *i.e.* the solvation shell around the ion, quantum mechanically, while the environment consisting of further solvent molecules is described by molecular mechanical potentials. By this scheme, the complicated many-body contributions as well as the polarization effects within the solvation sphere of the ion can be reliably included.

For studies on preferential solvation of ions in aqueous ammonia solution, Born–Oppenheimer *ab initio* QM/MM molecular dynamics simulations have been successfully applied to Li^+,[45] Na^+[46] and Mg^{2+}.[47] The results from QM/MM simulations have provided more reliable geometrical arrangements of the solvated ion structures, and they have reflected ligand preferences in agreement with the chemical concepts of Lewis acid–base interactions. The QM/MM simulations have clearly shown the importance of non-additive contributions for the description of the structural properties of solvated ions in such a solvent mixture. Based on the principle of hard and soft acids and bases (HSAB),[48–51] hard acids will prefer to coordinate to hard bases and soft acids will prefer to coordinate to soft bases. Li^+, Na^+ and Mg^{2+} are classified as "hard" ions and are thus expected to prefer the "harder" H_2O over the "softer" NH_3 as ligand. The QM/MM simulations have shown this preference for H_2O in agreement with the qualitative expectation according to the HSAB model.

In the present work, a Born–Oppenheimer *ab initio* QM/MM molecular dynamics simulation was carried out for Ca^{2+} in 18.4% aqueous ammonia solution. Ca^{2+} is one of the most important ions involved in many biological processes.[52,53] Nevertheless, the structural details of this ion, such as the hydration numbers, from both experimental and theoretical investigations, are still in doubt. Experiments reported hydration numbers of Ca^{2+} in the range 6–10,[16,54–56] while classical and QM/MM molecular dynamics simulations predicted values of 8–10,[40,57–59] 7.6,[60] and 8.3.[40] The observed variation in the experimental hydration numbers is strongly related to the concentration: they increase from ~6 to ~10 as the molality decreases from 4.5 to 1.[16] For the coordination numbers of Ca^{2+} in liquid ammonia, early MC simulations reported 9 and 8.2, as observed from pair and pair plus three-body correction simulations, respectively.[61] No structural properties for this ion in aqueous ammonia solution have been reported so far and therefore they are the main subject of interest in this paper.

2. Methods

By the technique of Born–Oppenheimer *ab initio* dynamics, the system is partitioned into a part described by quantum mechanics and another part treated by means of molecular mechanics. The total interaction energy of the system can be written as

$$E_{\text{total}} = \langle \Psi_{\text{QM}} | \hat{H} | \Psi_{\text{QM}} \rangle + E_{\text{MM}} + E_{\text{QM/MM}}. \quad (3)$$

The interactions within the solvation sphere of Ca^{2+} are considered as the active site (the QM region) and treated by Born–Oppenheimer *ab initio* Hartree–Fock quantum mechanical calculations using LANL2DZ basis sets,[62,63] while the interactions within the MM region and between the QM and MM regions are described by classical pair potentials. The LANL2DZ basis sets were selected as a reasonable compromise between the quality of the simulation results and the requirement of CPU time.[40–42,44–47,64] During the simulation, the exchange of solvent molecules between the QM and MM regions can occur frequently. In this case, the forces acting on each particle in the system are switched according to which region the ligand is entering or leaving and can be defined as:

$$F_i = S_m(r)F_{\text{QM}} + (1 - S_m(r))F_{\text{MM}}, \quad (4)$$

where F_{QM} and F_{MM} are quantum mechanical and molecular mechanical forces, respectively. $S_m(r)$ is a smoothing function,[65]

$$\begin{aligned} S_m(r) &= 1, && \text{for } r \le r_1, \\ S_m(r) &= \frac{(r_0^2 - r^2)^2 (r_0^2 + 2r^2 - 3r_1^2)}{(r_0^2 - r_1^2)^3}, && \text{for } r_1 < r \le r_0, \\ S_m(r) &= 0, && \text{for } r > r_0, \end{aligned} \quad (5)$$

where r_1 and r_0 are the distances characterizing the beginning and end of the QM region. $S_m(r)$ ensures a continuous change of forces in the transition between the QM and MM regions.

For interactions inside the MM and between the QM and MM regions, flexible models, which describe inter- and intramolecular interactions, have been employed for water[66,67] and ammonia.[68] The pair potential function for water–ammonia interactions was adopted from Tanabe *et al.*[69] The pair potential function for Ca^{2+}–H_2O interactions was obtained from our previous work.[40] The pair potential function for Ca^{2+}–NH_3 interactions was newly constructed in the present work using the DZV+(d,p) basis set for NH_3[62] and the Los Alamos ECP plus DZ basis set for Ca^{2+}.[63] These basis sets are consistent with those used in the construction of the Ca^{2+}–H_2O potential. 1400 Hartree–Fock interaction energy points for various Ca^{2+}–NH_3 configurations, obtained from Gaussian94[70] calculations, were fitted to the analytical form of

$$\Delta E_{Ca^{2+}-NH_3} = \sum_{i=1}^{3} \left(\frac{A_{ic}}{r_{ic}^5} + \frac{B_{ic}}{r_{ic}^8} + C_{ic}\exp(-D_{ic}r_{ic}) + \frac{q_i q_c}{r_{ic}} \right) \quad (6)$$

where A, B, C and D are the fitting parameters (see Table 1), r_{ic} denotes the distances between Ca^{2+} and the ith atom of ammonia and the q are the atomic net charges. The charges on Ca^{2+}, N and H of ammonia were set to 2.0, −0.8022 and 0.2674, respectively.

A classical molecular mechanical (pairwise additive approximation) molecular dynamics simulation was performed first, followed by the combined QM/MM molecular dynamics simulation starting from the equilibrium configuration obtained by the classical simulation. Many-body interactions are considered most significant at short range between strongly interacting particles. For ions in solution, the suitable QM size is the sphere including all ligands within the complete solvation sphere of the ions. However, the use of such a QM region, particularly for some strongly interacting ions, is too time-consuming. The QM region is the most expensive computational part and hence the size of it has to be a compromise

Table 1 Optimized parameters of the analytical pair potential for the interaction of ammonia with Ca^{2+} (interaction energies in kcal mol^{-1} and distances in Å)

Pair	A/kcal mol^{-1} Å^5	B/kcal mol^{-1} Å^8	C/kcal mol^{-1}	D/Å^{-1}
Ca–N	−11757.345	16203.122	82683.774	2.7866018
Ca–H	−1043.5280	2957.6223	−762.25558	1.4852236

between the reliability of results and the available computational resources. As can be seen from the Ca–(N + O) radial distribution function obtained by the classical simulation (Fig. 1), the second minimum of the RDF peak is located around 5.9 Å. Within this region, there are about 27 water and 5 ammonia molecules, which is a prohibitively large number for performing a QM/MM simulation. To decrease the QM size, the second maximum of the Ca–(N + O) peak around 4.75 Å, is an alternative choice. There are about 14 water and 3 ammonia molecules located within this region, leading to 12–16 min to compute the forces in each QM/MM step (on a DEC Alpha XP1000 workstation). This is acceptable and, therefore, the QM region was set to a diameter of 9.6 Å in the simulation, assuming that this size would be large enough to ensure a smooth convergence of the quantum mechanical forces to the pair potential forces beyond the QM region.

The classical and combined QM/MM simulations were performed in a canonical ensemble at 293 K, with a time step size of 0.2 fs. This canonical ensemble was realized by coupling to an external temperature bath. The basic cube, with a length of 18.56 Å, contained one Ca^{2+}, 37 ammonia and 163 water molecules, assuming the experimental density of 18.4% aqueous ammonia solution at the given temperature (0.9398 g cm^{-3}). The reaction-field method was employed for the treatment of long-range interactions.[71] This method also implies a compensation of the electrical non-neutrality of the basic box. The classical pair potential simulation started from an equilibrium configuration obtained from a previous simulation for Mg^{2+} in aqueous ammonia solution.[47] The system was equilibrated for 60 000 steps, and the simulation was continued for another 100 000 steps to collect configurations every 10th step. The QM/MM simulation started with a re-equilibration for 20 000 steps, followed by another 30 000 steps to collect configurations every 5th step. The 6 ps interval of our QM/MM simulation can be considered long enough since it has been shown that even a 2 ps simulation can deliver most of the structural and dynamical properties of similar solutions.[39,41,42,44] In particular, for Ca^{2+} in water, the QM/MM-HF simulation has shown that the exchange of a water molecule between the first and second hydration shells of the ion takes about 2 ps.[72] The switching function of eqn. (4) was applied within an interval of 0.2 Å (*i.e.*, in eqn. (5), $r_l = 4.6$ and $r_0 = 4.8$ Å).

3. Results and discussion

Fig. 1 shows the overall Ca–(N + O) and Ca–H (from both water and ammonia molecules) RDFs and their corresponding integration numbers, obtained from both classical and combined QM/MM simulations. The classical simulation gives a sharp first Ca–(N + O) peak at 2.60 Å and the first solvation shell is well separated from the second one, leading to a coordination number of 9.7. In the QM/MM simulation, a pronounced first Ca–(N + O) peak with two maxima at 2.45 and 2.63 Å is observed. The first solvation shell is well separated from the second one, giving a coordination number of 7.2. The second Ca–(N + O) peak in the pair potential simulation is less pronounced with the maximum at around 4.75 Å. In contrast to this, in the QM/MM simulation the second peak is well defined with the maximum at around 4.53 Å, consisting of about 18 ligands. In order to discuss the composition of the solvation shell of Ca^{2+}, the Ca–H_2O and Ca–NH_3 RDFs and their corresponding integration numbers are plotted separately in Fig. 2 and 3, respectively. The characteristics of the Ca–H_2O and Ca–NH_3 RDFs obtained from this work are summarized in Table 2. In the Ca–H_2O RDFs, the first Ca–O and Ca–H peaks in the QM/MM simulation have their maxima at shorter distances of 2.44 and 3.06 Å, compared to the corresponding values of 2.48 and 3.20 Å of the pair potential

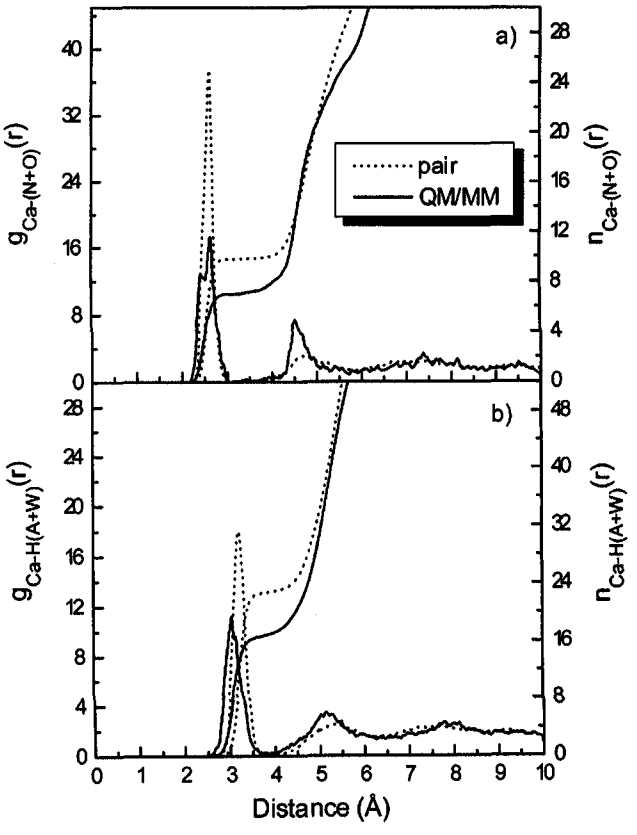

Fig. 1 (a) Ca–(N + O) and (b) Ca–H(A + W) radial distribution functions and their corresponding integration numbers.

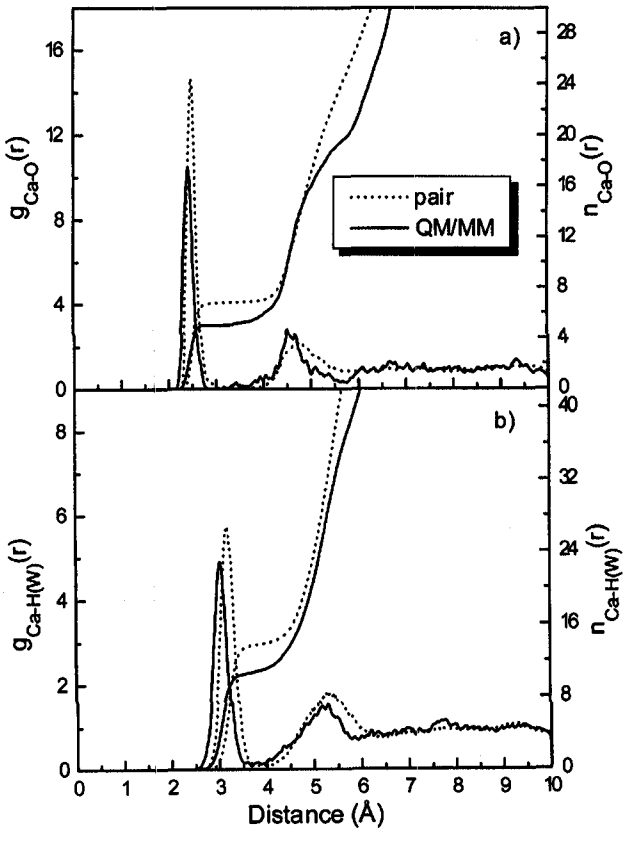

Fig. 2 (a) Ca–O and (b) Ca–H(W) radial distribution functions and their corresponding integration numbers.

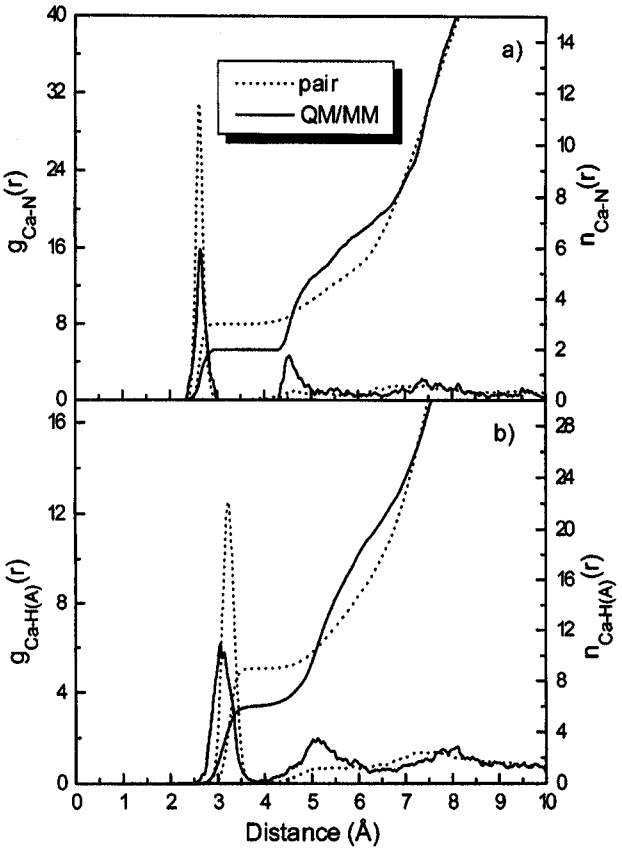

Fig. 3 (a) Ca–N and (b) Ca–H(A) radial distribution functions and their corresponding integration numbers.

simulation, and consist of 5.2 and 6.7 water molecules, respectively. In both classical and QM/MM simulation, the second Ca–H_2O peaks are recognizable, as can be seen from the distribution of water molecules within this shell. In the Ca–NH_3 RDFs, the pair potential simulation produces a very sharp first Ca–N peak centered at 2.61 Å, giving a coordination number of 3, and no second peak is observed. In the QM/MM simulation, a less pronounced first Ca–N peak is located at 2.64 Å, corresponding to 2 ammonia molecules. A second peak is also well recognized with a maximum around 4.54 Å, indicating the participation of both water and ammonia molecules in the second solvation shell of Ca^{2+}. To characterize the two maxima appearing in the first Ca–(N + O) peak of QM/MM simulation, *ab initio* geometry optimizations of Ca^{2+}–H_2O and Ca^{2+}–NH_3 complexes, using the DZV+(d,p) basis set for ligands and the Los Alamos ECP plus DZ basis set for Ca^{2+}, have been performed. The optimal Ca–O and Ca–N distances are 2.37 and 2.52 Å, which correspond to the first Ca–(N + O) peak obtained by the QM/MM simulation for the distribution of water and ammonia molecules, respectively. It is plausible that the larger NH_3 ligands would experience more steric hindrance and hence be located farther away from the ion than the smaller H_2O molecules. The global minima for Ca^{2+}–NH_3 and Ca^{2+}–H2O interactions (−54.8 and −49.6 kcal mol^{-1} after *ab initio* geometry optimizations) would imply that Ca^{2+} binds more strongly to NH_3 than to H_2O. However, in the case of a multi-solvated ion with non-ideal orientations one has to consider that repulsive forces for geometries deviating from the dipole-oriented configuration are much stronger in the case of Ca^{2+}–NH_3 interactions than in the case of Ca^{2+}–H_2O interactions.[45]

Fig. 4 shows the probability distributions of the solvation numbers of Ca^{2+}, calculated up to the second minimum of the Ca–(N + O) RDFs. In the classical simulation, about 25–33 ligands, namely 21–27 water and 4–6 ammonia molecules, are located within the solvation sphere. A lower solvation number of 19–25 is observed in the QM/MM simulation, corresponding to 15–19 water and 4–6 ammonia molecules. The distributions of coordination numbers within the first and the second solvation shell of Ca^{2+} are plotted separately in Fig. 5. In the classical simulation, the first solvation shell of Ca^{2+} prefers a coordination number of 10 (followed by 9 to a lesser extent), consisting of 7 (and 6 to a lesser extent) water and 3 ammonia molecules. The second solvation shell favors a coordination number of 20 (in addition to 19 and 18 in comparable amounts). In the QM/MM simulation, the first solvation shell of Ca^{2+} prefers a coordination number of 7 (followed by 8 and 6 in decreasing amounts), consisting of 5 (and 6 in a smaller amount) water and 2 (and 1 in smaller

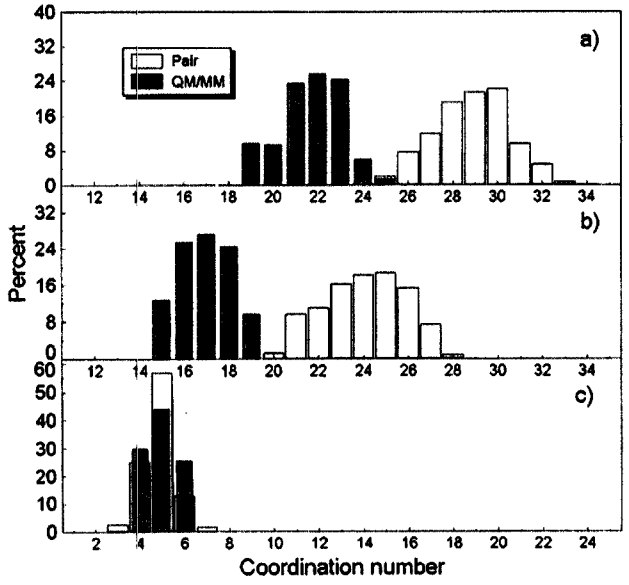

Fig. 4 Coordination number distributions, calculated up to the second minimum of the Ca^{2+}–ligand RDFs: (a) Ca^{2+}–(H_2O+NH_3), (b) Ca^{2+}–H_2O and (c) Ca^{2+}–NH_3.

Table 2 Comparison of solvation parameters for Ca^{2+} in 18.4% aqueous ammonia solution, obtained from classical and QM/MM simulations (r_{max1}, r_{max2}, r_{min1} and r_{min2} denote the first maximum, the second maximum, the first minimum and the second minimum of the radial distribution functions in Å, and n_{min1} and n_{min2} are the average numbers of ligands obtained by integration up to r_{min1} and r_{min2}, respectively)

	r_{max1}	r_{min1}	n_{min1}	r_{max2}	r_{min2}	n_{min2}	Method
Ca–O	2.48	3.09	6.7	4.70	6.04	27.3	Classical MD
	2.44	2.80	5.2	4.53	5.72	19.7	QM/MM MD
Ca–H(W)	3.20	3.75	13.7	5.26	6.34	58.7	Classical MD
	3.06	3.64	10.6	5.28	5.91	39.9	QM/MM MD
Ca–N	2.61	3.06	3.0	—	—	—	Classical MD
	2.64	2.97	2.0	4.54	5.08	4.9	QM/MM MD
Ca–H(A)	3.24	3.83	9.0	—	—	—	Classical MD
	3.06	3.79	6.0	5.15	6.22	19.2	QM/MM MD

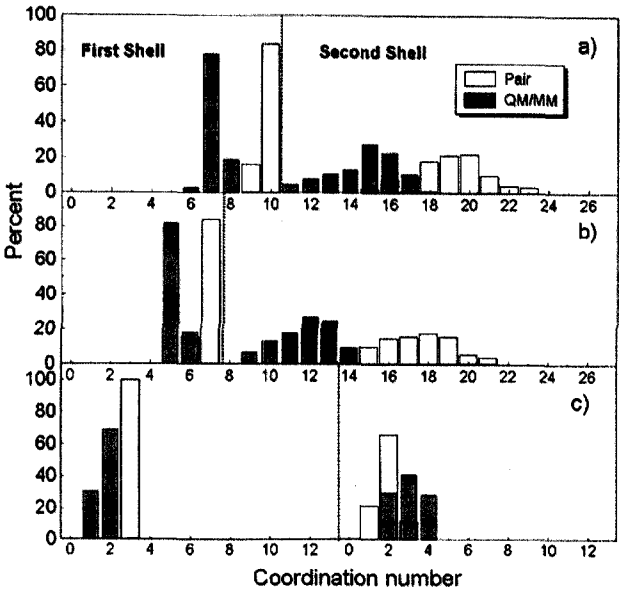

Fig. 5 Coordination number distributions, calculated within the first and the second solvation shell of the Ca^{2+}: (a) Ca^{2+}–(H_2O+NH_3), (b) Ca^{2+}–H_2O and (c) Ca^{2+}–NH_3.

amount) ammonia molecules. The second solvation shell prefers a coordination number of 15 (in addition to 16, 14, 17, 13, 12, and 11 in smaller amounts), made up of 12 (followed by 13, 11, 10, 14 and 9 in decreasing amounts) water and 3 (in addition to 2 and 4 in equivalent amounts) ammonia molecules.

According to the composition of the solution, which contained one calcium ion, 37 ammonia and 163 water molecules, the statistical average distribution of ligands around Ca^{2+} would have been approximately 4.4 : 1 for water and ammonia, respectively. The QM/MM simulation depicts a water-to-ammonia ratio of 5.2 : 2 (2.6 : 1). With respect to the HSAB principle,[48–51] Ca^{2+} is not a really "hard" ion (*e.g.* compared to Mg^{2+}) and is not expected, therefore, to show a preference for the "harder" H_2O over the "softer" NH_3. From the results obtained in this work, it seems that Ca^{2+} even prefers the NH_3 molecules as first-shell ligand. When taking into account the full solvation sphere including the first and second solvation shells of Ca^{2+}, the corresponding water-to-ammonia ratio obtained by the QM/MM simulation changes to 5 : 1, however, which is again not too different from the statistical average.

Fig. 6 presents the O–Ca–O, N–Ca–N and O–Ca–N angular distributions, calculated up to the first minimum of the Ca–(N + O) RDFs. From both classical and combined QM/MM simulations, the solvation shell structure of Ca^{2+} is predicted to be approximately polyhedral, as can be seen from the distributions of O–Ca–O, N–Ca–N and O–Ca–N peaks. For this structure, the ammonia molecules are arranged in a non-nearest-neighbor pattern. In order to investigate the influence of many-body contributions on the preferential orientations of ligands around the solvation sphere of Ca^{2+}, the angle θ, defined by the Ca···O axis and the dipole vector of the ligands, has been used. The dipole-oriented arrangements of water and ammonia molecules within the first solvation shell of the ion are given in Fig. 7. Both classical and combined QM/MM simulations indicate that the ammonia molecules stick more rigidly to the dipole-oriented arrangement than the water molecules. This can be ascribed to the higher binding energy of Ca^{2+} to NH_3 than to H_2O. In the first solvation shell of Ca^{2+}, the QM/MM simulation indicates a more flexible dipole-oriented arrangement of both water and ammonia molecules than the classical simulation. In the second solvation shell of Ca^{2+}, the effects of the ion on the orientation of the ligands are not much different between the classical and the combined QM/MM simulations.

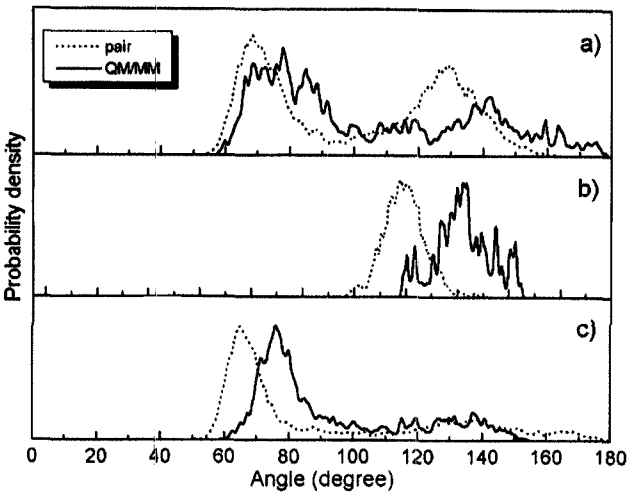

Fig. 6 Distributions of (a) O–Ca–O; (b) N–Ca–N and (c) O–Ca–N angles, calculated up to the first minimum of Ca–(N + O) RDFs.

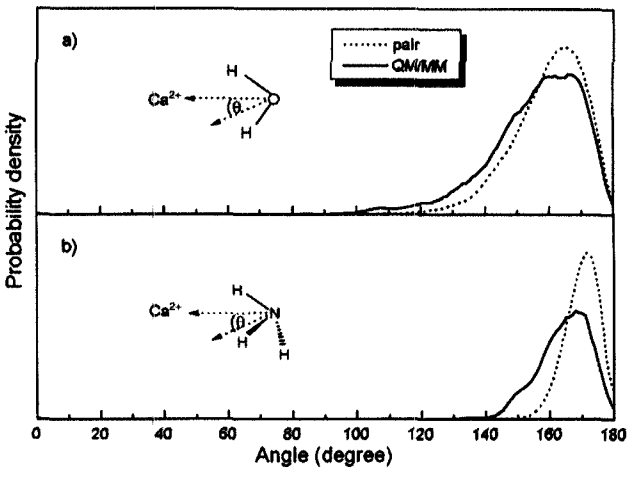

Fig. 7 Distributions of θ within the first solvation shell of Ca^{2+}. (a) water and (b) ammonia.

The main advantage of applying combined QM/MM simulation is to correct the effects of many-body contributions within the solvation shell of Ca^{2+}, which are mostly due to polarization effects. These effects of polarization are an essential difference to the molecular mechanical potentials using fixed partial charges for each atom in the system. For strong ion–ligand interaction systems, the changes in charge distributions within the interacting molecules are substantial and vary considerably during the molecular movements. According to our previous studies for Na^+ [46] and Mg^{2+},[47] ligands inside the QM region are strongly polarized by Ca^{2+}. This leads to higher Mulliken atomic charges of the ligand atoms by about 35% and 28% for water and ammonia, respectively (*i.e.*, N and O atoms become more negative and H atoms more positive).

In addition to the correct description of polarization effects, *ab initio* calculations can be used to obtain an estimate of charge transfer for the Lewis acid–base complexes.[73,74] This makes the *ab initio* treatment even more significant, as it allows one to distinguish between the effects of polarization, where *charge within the solvent molecules is redistributed while the* total charge remains constant, and charge transfer, where charge is exchanged between the solvent molecules and the ion. The effects of charge transfer can be expected to play an important role in the case of doubly or even higher charged ions. Based on the Mulliken population analysis, the average

charge on Ca^{2+} is +1.71, compared to the constant value of +2.0 employed in the pair potential simulation, implying that the use of this charge on Ca^{2+} in the classical simulation results in an over-stabilization for short-range Ca^{2+}–ligand interactions. A classical simulation with the reduced charge on Ca could be a first approach to correct this error, but it could never reach the quality of the QM/MM approach, where the Ca charge is corrected dynamically according to the structural changes of the solvate.

Our QM/MM results concerning the preferential solvation of Ca^{2+} in aqueous ammonia solution can provide some insight into the feature of Ca^{2+}–ligand complexes in biological systems. Such complexes have both N- and O- binding ligands of various types. In this respect, the coordinating oxygen and nitrogen atoms of water and ammonia molecules can be seen as models representing some oxygen- or nitrogen-containing ligands (*e.g.* functional groups of proteins and other biomolecules). According to the crystal structures known for calcium–protein and calcium–nucleic acid complexes,[75] Ca^{2+} shows coordination numbers of 6, 7 or 8. In most cases, Ca^{2+} prefers to bind to oxygen rather than to nitrogen. In particular for the coordination number of 7, the Ca^{2+} coordination in crystal structures containing $Ca^{2+}\cdots X$ (X = O and N) can be 7O, 6O/1N and 5O/2N. This preference is in good agreement with the preferential solvation of the ion as observed in our QM/MM simulation. The correct description of calcium binding in complexes is very important since such complexes require very specific and selective conformations in order to respond appropriately to biological signals.[76,77] For example, the interactions of regulatory proteins such as calmodulin with other proteins are strongly determined by the specific binding situation of Ca^{2+}.[78]

4. Conclusion

The QM/MM simulation technique has provided detailed data for the solvation structure of Ca^{2+} in 18.4% aqueous ammonia solution. This technique has predicted considerably lower coordination numbers than the classical pair potential simulation, proving once more the important role of non-additive contributions and mutual polarization effects for a correct description of solvated ions.

Acknowledgements

Financial support for this work by the Thailand Research Fund (Grant No. PDF/28/2543) is gratefully acknowledged. BMR acknowledges support by the Austrian Science Foundation (FWF Project 13644 TPH).

References

1 V. Gutmann, *The Donor-Acceptor Approach to Molecular Interactions*, Plenum Press, New York, 1978.
2 Y. Marcus, *Ion Solvation*, Wiley, New York, 1985.
3 V. A. Sajeevkumar and S. Singh, *J. Mol. Struct.*, 1996, **382**, 101.
4 D. Jamróz, M. Wójcik and J. Lindgren, *Spectrochim. Acta, Part A*, 2000, **56**, 1939.
5 E. Hawlicka and D. Swiatla-Wojcik, *J. Mol. Liq.*, 1998, **78**, 7.
6 E. Kamieńska-Piotrowicz and J. Stangret, *J. Mol. Struct.*, 1995, **344**, 69.
7 H. D. Pranowo and B. M. Rode, *Chem. Phys.*, 2001, **263**, 1.
8 S. Vizoso and B. M. Rode, *Chem. Phys.*, 1996, **213**, 77.
9 B. M. Rode and Y. Tanabe, *J. Chem. Soc., Faraday Trans.*, 1988, **2**, 1779.
10 R. D. Mountain, *Int. J. Thermophys.*, 2001, **22**, 101.
11 M.-C. Bellissent-Funel and G. W. Neilson, *The Physics and Chemistry of Aqueous Ionic Solutions*, Reidel, Dordrecht, 1987.
12 G. W. Neilson, *Pure Appl. Chem.*, 1988, **60**, 1797.
13 G. W. Neilson and J. E. Enderby, *Adv. Inorg. Chem.*, 1989, **34**, 195.
14 G. W. Neilson and R. H. Tromp, *Annu. Rep. Phys. Chem. C*, 1991, **88**, 45.
15 M. Magini, G. Licheri, G. Paschina and G. Piccaluga, *X-ray Diffraction of Ions in Aqueous Solutions: Hydration and Complex Formation*, CRC Press, Boca Raton, FL, 1988.
16 N. A. Hewish, G. W. Neilson and J. E. Enderby, *Nature.*, 1982, **297**, 138.
17 I. Howell and G. W. Neilson, *J. Phys.: Condens. Matter*, 1996, **8**, 4455.
18 S. Kheawsrikul, S. V. Hannongbua, S. Kokpol and B. M. Rode, *J. Chem. Soc., Faraday Trans.*, 1989, **85**, 643.
19 S. Kheawsrikul and S. Hannongbua, *Z. Naturforsch. A*, 1991, **46**, 111.
20 K. Kistenmacher, H. Popkie and E. Clementi, *J. Chem. Phys.*, 1974, **61**, 799.
21 R. H. Beaumont, H. Chihara and J. A. Morrison, *Proc. Phys. Soc.*, 1961, **78**, 1462.
22 E. Ermakova, J. Solca, H. Huber and D. Marx, *Chem. Phys. Lett.*, 1995, **246**, 204.
23 M. M. Probst, E. Spohr, K. Heinzinger and P. Bopp, *Mol. Simul.*, 1991, **7**, 43.
24 I. Ortega-Blake, O. Novaro, A. Lés and S. Rybak, *J. Chem. Phys.*, 1982, **76**, 5405.
25 T. P. Lybrand and P. A. Kollman, *J. Chem. Phys.*, 1985, **83**, 2923.
26 E. Clementi, H. Kistenmacher, W. Kolos and S. Romano, *Theor. Chim. Acta.*, 1980, **55**, 257.
27 L. A. Curtiss, J. W. Halley, J. Hautman and A. Rahman, *J. Chem. Phys.*, 1987, **86**, 2319.
28 M. I. Bernal-Uruchurtu and I. Ortega-Blake, *J. Chem. Phys.*, 1995, **103**, 1588.
29 A. Warshel and M. Levitt, *J. Mol. Biol.*, 1976, **103**, 227.
30 U. C. Singh and P. A. Kollman, *J. Comput. Chem.*, 1986, **7**, 718.
31 M. J. Field, P. A. Bash and M. Karplus, *J. Comput. Chem.*, 1990, **11**, 700.
32 J. Åqvist and A. Warshel, *Chem. Rev.*, 1993, **93**, 2523.
33 R. V. Stanton, D. S. Hartsough and K. M. Merz, Jr., *J. Comput. Chem.*, 1995, **16**, 113.
34 R. P. Muller and A. Warshel, *J. Phys. Chem.*, 1995, **99**, 17516.
35 J. Gao, *Rev. Comput. Chem.*, 1996, **7**, 119.
36 M. A. Thompson, *J. Phys. Chem.*, 1996, **100**, 14492.
37 P. L. Cummins and J. E. Gready, *J. Comput. Chem.*, 1997, **18**, 1496.
38 J. Gao, P. Amara, C. Alhambra and M. J. Field, *J. Phys. Chem. A*, 1998, **102**, 4714.
39 T. Kerdcharoen, K. R. Liedl and B. M. Rode, *Chem. Phys.*, 1996, **211**, 313.
40 A. Tongraar, K. R. Liedl and B. M. Rode, *J. Phys. Chem. A*, 1997, **101**, 6299.
41 A. Tongraar, K. R. Liedl and B. M. Rode, *Chem. Phys. Lett.*, 1998, **286**, 56.
42 A. Tongraar, K. R. Liedl and B. M. Rode, *J. Phys. Chem. A*, 1998, **102**, 10340.
43 G. W. Marini, K. R. Liedl and B. M. Rode, *J. Phys. Chem. A*, 1999, **103**, 11387.
44 T. Kerdcharoen and B. M. Rode, *J. Phys. Chem. A*, 2000, **104**, 7073.
45 A. Tongraar and B. M. Rode, *J. Phys. Chem. A*, 1999, **103**, 8524.
46 A. Tongraar and B. M. Rode, *J. Phys. Chem. A*, 2001, **105**, 506.
47 A. Tongraar, K. Sagarik and B. M. Rode, *J. Phys. Chem. B*, 2001, **105**, 10559.
48 G. Schwarzenbach, *Experentia Suppl.*, 1956, **5**, 163.
49 S. Ahrland, J. Chatt and N. Davies, *Quart. Rev.*, 1958, **12**, 265.
50 R. G. Pearson, *Struct. Bonding*, 1993, **80**, 1.
51 L. Komorowski, *Struct. Bonding*, 1993, **80**, 45.
52 D. E. Clapham, *Cell*, 1995, **80**, 259.
53 W. J. Chazin, *Nat. Struct. Biol.*, 1995, **2**, 707.
54 S. Cummings, J. E. Enderby and R. A. Howe, *J. Phys. C*, 1980, **13**, 1.
55 G. Licheri, G. Piccaluga and G. Pinna, *J. Chem. Phys.*, 1976, **64**, 2437.
56 T. Yanaguchi, S. Heyashi and H. Ohtaki, *Inorg. Chem.*, 1989, **28**, 2434.
57 S. Obst and H. Bradaczek, *J. Phys. Chem.*, 1996, **100**, 15677.
58 S. G. Kallko, G. Sesé and J. A. Padró, *J. Chem. Phys.*, 1996, **104**, 9578.
59 F. M. Floris, M. Persico, A. Tani and J. Tomasi, *Chem. Phys. Lett.*, 1994, **227**, 126.
60 C. F. Schwenk, H. H. Loeffler and B. M. Rode, *J. Chem. Phys.*, 2001, **115**, 10808.
61 W. Sidhisoradej, S. Hannongbua and D. Rufforo, *Z. Naturforsch. A*, 1998, **53**, 208.

62 T. H. Dunning, Jr and P. J. Hay, *Modern Theoretical Chemistry*, ed. H. F. Schaefer III, Plenum Press, New York, 1976.
63 P. J. Hay and W. R. Wadt, *J. Chem. Phys.*, 1985, **82**, 270.
64 A. Tongraar, PhD Thesis, University of Innsbruck, Innsbruck, Austria, 1998.
65 B. R. Brooks, R. E. Bruccoleri, B. D. Olafson, D. J. States, S. Swaminathan and M. Karplus, *J. Comput. Chem.*, 1983, **4**, 187.
66 P. Bopp, G. Jancsó and K. Heinzinger, *Chem. Phys. Lett.*, 1983, **98**, 129.
67 F. H. Stillinger and A. Rahman, *J. Chem. Phys.*, 1978, **68**, 666.
68 S. Hannongbua, T. Ishida, E. Spohr and K. Heinzinger, *Z. Naturforsch. A*, 1988, **43**, 572.
69 Y. Tanabe and B. M. Rode, *J. Chem. Soc., Faraday Trans. 2*, 1988, **84**, 679.
70 M. J. Frisch, G. W. Trucks, H. B. Schlegel, P. M. W. Gill, B. G. Johnson, M. A. Robb, J. R. Cheeseman, T. A. Keith, G. A. Peterson, J. A. Montgomery, K. Raghavachari, M. A. Al-Laham, V. G. Zakrzewski, J. V. Ortiz, J. B. Foresman, J. Cioslowski, B. B. Stafanov, A. Nanayakkara, M. Challacombe, C. Y. Peng, P. Y. Ayala, W. Chen, M. W. Wong, J. L. Andres, E. S. Replogle, R. Gomperts, R. L. Martin, D. J. Fox, J. S. Binkley, D. J. Defrees, J. Baker, J. P. Stewart, M. Head-Gordon, C. Gonzalez and J. A. Pople, *GAUSSIAN 94*, Gaussian, Inc., Pittsburgh, PA, 1995.
71 D. J. Adams, E. H. Adams and G. J. Hills, *Mol. Phys.*, 1979, **38**, 387.
72 C. F. Schwenk, H. H. Loeffler and B. M. Rode, submitted.
73 R. S. Mulliken and W. B. Person, *Molecular Complexes*, Wiley, New York, 1969.
74 Y. Mo and J. Gao, *J. Phys. Chem. A*, 2001, **105**, 6530.
75 A. K. Katz, J. P. Glusker, S. A. Beebe and C. W. Bock, *J. Am. Chem. Soc.*, 1996, **118**, 5752.
76 C. W. Heizmann and W. Hunziker, *Trends Biochem. Sci.*, 1991, **16**, 98.
77 M. R. Celio, T. Pauls and B. Schwaller, *Guidebook to the Calcium-Binding Proteins*, Oxford University Press, Oxford, 1996.
78 C. B. Klee and T. C. Vaenaman, *Adv. Protein Chem.*, 1982, **35**, 213.